Mon. Not. R. Astron. Soc. **346,** 555–564 (2003)

Contribution to the search for binaries among Am stars – V. Orbital elements of eight short-period spectroscopic binaries

J.-M. Carquillat,[1] N. Ginestet,[1] J.-L. Prieur[1★] and Y. Debernardi[2]

[1]*UMR 5572 d'Astrophysique, Observatoire Midi-Pyrénées – CNRS, 14, Avenue Edouard Belin, 31400 Toulouse, France*
[2]*Institut d'Astronomie de l'Université de Lausanne, 1290 Chavannes-des-Bois, Switzerland*

Accepted 2003 August 11. Received 2003 July 21; in original form 2003 May 26

ABSTRACT

We present the results of a radial-velocity study of eight Am stars (HD 341, 55822, 61250, 67317, 93991, 162950, 224890 and 225137) observed at Observatoire de Haute-Provence with the CORAVEL instrument. We find that these systems are single-line spectroscopic binaries whose orbital elements are determined for the first time.

Key words: binaries: spectroscopic – stars: fundamental parameters.

1 INTRODUCTION

This paper is the fifth of a series devoted to the search and study of spectroscopic binaries (SBs) among a sample of chemically peculiar stars of type Am. This work was carried out at the Haute-Provence Observatory using the CORAVEL instrument mounted at the Cassegrain focus of the 1-m Swiss telescope. Papers I–IV concerned the most peculiar binaries first detected in the sample, such as double-lined and multiple systems; see Ginestet & Carquillat (1998, Paper I), Carquillat, Ginestet & Prieur (2001, Paper II), Carquillat et al. (2002, Paper III) and Ginestet et al. (2003, Paper IV). This paper is devoted to the radial-velocity (RV) study of eight single-lined (SB1) short-period ($P \leqslant 10$ d) SBs, namely HD 341, 55822, 61250, 67317, 93991, 162950, 224890 and 225137. A forthcoming paper will deal with statistics about the whole programme.

All these stars were listed in the 'Third catalogue of Am stars with known spectral types' (Hauck 1986), the main source from which we constituted our sample.

In Section 2, we present our RV observations and the orbital elements we computed. We then give some complementary information about the spectral classification of those systems in Section 3. In Section 4 we derive some physical parameters deduced from photometric indices, using *Hipparcos* parallaxes and theoretical evolutionary tracks. We also estimate the minimum masses and separations of the companions. Finally, we discuss the occurrence of rotation-revolution synchronism among these systems.

2 OBSERVATIONS AND DERIVATION OF ORBITAL ELEMENTS

To our knowledge, among these eight stars, only HD 225137 was previously detected as having a variable radial velocity (Grenier et al. 1999). Our observations were performed during the period 1992–1999 with the CORAVEL instrument (Baranne, Mayor & Poncet 1979), a spectrophotometer that allows measurements of heliocentric RVs by performing a cross-correlation of the stellar spectrum with a physical mask placed in the focal plane of the spectrograph. For HD 224890, we also added three measurements made by Benz & Mayor in 1980–1982 during the first determinations of $v \sin i$ values for the Am stars with CORAVEL.

40 to 70 observations for each object have been carried out. These data were kindly reduced and input into the Geneva RV data base (Udry, Mayor & Queloz 1999) by S. Udry. For each star, the mean internal standard error strongly depends upon its rotational velocity $v \sin i$. That error varies from about 0.5 km s^{-1} for $v \sin i \approx 10$ km s^{-1} to about 1.1 km s^{-1} for $v \sin i \approx 25$ km s^{-1}. As an illustration, we give two examples of correlation dips, for HD 93991 ($v \sin i = 26$ km s^{-1}), and for HD 162950 ($v \sin i = 9$ km s^{-1}), in Fig. 1. For all systems, the secondary dip from the spectroscopic companion could not be detected.

The orbital elements of the eight stars (Table 1) were subsequently calculated by applying the least-squares program BS1 (Nadal et al. 1979, revised by JLP) to the observed RVs. Those RVs, and the corresponding (O − C) residuals are given in Tables 2–9, and the computed RV curves in Figs 2 and 3. For each of those SBs, the standard deviation of the residuals, $\sigma_{(O-C)}$ is consistent with the RV mean error, which indicates the absence of detectable spectroscopic third bodies in those systems. Note that HD 61250, HD 67317 and HD 93991 have a circular orbit according to the statistical test of Lucy & Sweeney (1971). Hence, all the orbits of the binaries of our sample with $P < 5$ d are circularized.

3 NOTES FOR INDIVIDUAL SYSTEMS

In these notes, we report the classifications mentioned in Hauck's catalogue. For an Am star, let us recall that there are three spectral classifications k, h and ml, according to the spectral features that are used: K line of Ca II (k), Balmer lines (h), and metallic lines (ml).

HD 341. The Am star is the B component of the visual triple system STT 4256 = CCDM 00081+3123. Strömgren photometry is available. Classified A3(k) F0(h) F2(ml).

★E-mail: prieur@ast.obs-mip.fr

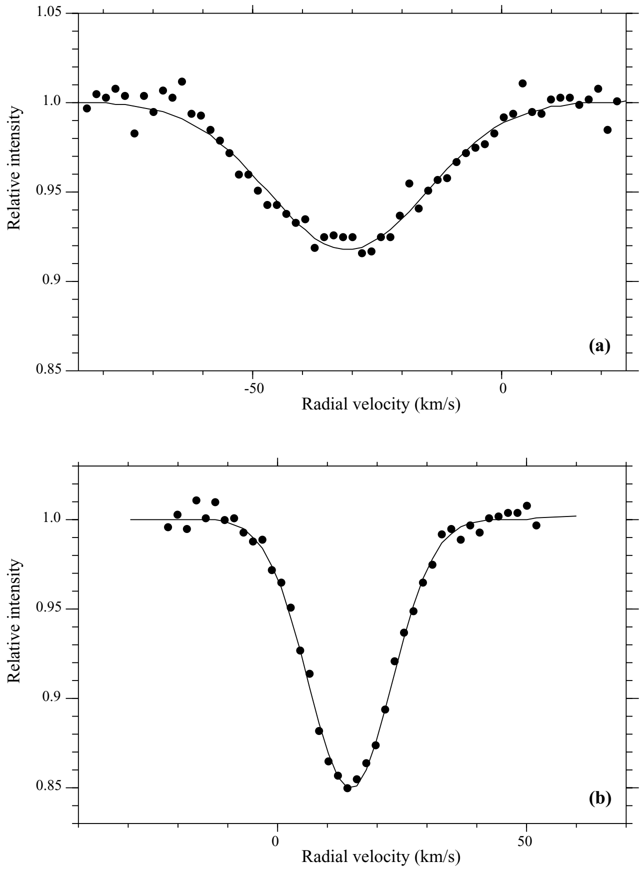

Figure 1. Examples of correlation dips obtained with CORAVEL: (a) HD 93991 and (b) HD 162950.

HD 55822. This star belongs to the system ADS 5922 AB = CCDM 07154+1904 AB. $\Delta m_{\mathrm{Hip}} = 3.2$, Sep. 2.2 arcsec. Strömgren photometry is available. Classification: A2(k) F2(h) F5(ml).

HD 61250. Visual double HEI 132 = WDS 07429+6517. $\Delta m_v = 1.4$, Sep. 0.5 arcsec. Strömgren and H_β photometry are available. Classification: A3(k) F3(h) F5(ml).

HD 67317. The star is ADS 6620 AB = CCDM 08102+5548 AB. $\Delta m_{\mathrm{Hip}} = 3.1$, Sep. 1.4 arcsec. Geneva photometry is available. Classification: A1(k) F1(h) F2(ml) (Hauck 1986); A2(k) A5(h) F3(ml) (Grenier et al. 1999).

HD 93991. Strömgren and H_β photometry are available. Classification: A8(k) F2(h) F3(ml).

HD 162950. Bright component of the visual double system CCDM 17525+2712. Strömgren, H_β, and Geneva photometry are available. Classification: A3(k) F4(ml) (Hauck 1986); A3(k) A7(h) F3(ml) (Grenier et al. 1999).

HD 224890. Geneva photometry is available. Classification: A1(k) F2(ml).

HD 225137. The star is HJ 1926 AD = CCDM 00039+5723 AD ($\Delta m_v = 6.0$). Geneva photometry is available. Classification: A3(k) F2(ml) (Hauck 1986); A3(k) A7(h) F2(ml) (Grenier et al. 1999).

4 PHYSICAL PARAMETERS AND DISCUSSION

4.1 Physical parameters of the primaries

For all the systems studied here, we detected the RV variations of the primary only. As seen in the previous section, six of these stars are also members of visual binary systems, with very faint companions: $\Delta m_v > 3$ for all systems, except for HD 61250. Hence we shall admit for all systems but HD 61250 that the photometric data (V, B–V, Strömgren indices, for example) practically concern only the primaries of the SB1s of our sample.

For HD 61250, photometric magnitudes of both components were obtained, in the Tycho system, by Fabricius & Makarov (2000). We deduce $(B{-}V)_{1,\mathrm{Tyc}} = 0.27$ and $(B{-}V)_{2,\mathrm{Tyc}} = 0.60$ for the components A and B, respectively. Converted to Johnson's system, this leads to $(B{-}V)_1 = 0.23$, $(B{-}V)_2 = 0.51$ and $\Delta m_V = 1.41$. Then, the primary of the visual system, the Am star, would have a temperature of about 7600 K, and the visual secondary could be a cooler dwarf star (∼F8V) with $T \approx 6200$ K (cf. calibrations of Schmidt-Kaler 1982 and Flower 1996).

Table 1. Orbital elements. In column 3, T_0 is the epoch of periastron passage, except for HD 61250, HD 67317, HD 93991 and HD 225137, for which T_0 corresponds to the ascending node passage.

Name	P d	T_0 (JD) 2400000+	ω deg.	e	K_1 km s^{-1}	V_0 km s^{-1}	$a_1 \sin i$ Gm	$f(m)$ M$_\odot$	$\sigma_{(O-C)}$ km s^{-1}
HD 341	6.24268	48941.63	299.1	0.010	32.46	−3.19	2.79	0.0221	0.46
	±0.00003	±0.32	±18.7	±0.003	±0.11	±0.08	±0.01	±0.0002	
HD 55822	5.12294	48673.60	70.6	0.122	40.20	30.87	2.81	0.0338	0.84
	±0.00003	±0.03	±2.0	±0.004	±0.18	±0.12	±0.01	±0.0005	
HD 61250	2.23024	48939.29	–	0.000	25.37	−5.43	0.78	0.00378	1.27
	±0.00002	±0.01	–	–	±0.27	±0.19	±0.01	±0.00012	
HD 67317	4.43324	49321.05	–	0.000	33.23	6.37	2.03	0.0169	0.69
	±0.00003	±0.01	–	–	±0.16	±0.11	±0.01	±0.0002	
HD 93991	3.20858	48675.01	–	0.000	16.46	−15.33	0.73	0.00149	1.01
	±0.00003	±0.01	–	–	±0.21	±0.14	±0.01	±0.00006	
HD 162950	10.04288	49153.90	257.9	0.205	11.87	7.03	1.60	0.00164	0.35
	±0.00017	±0.05	±1.6	±0.006	±0.07	±0.05	±0.01	±0.00004	
HD 224890	9.54640	48971.19	85.6	0.214	10.89	−8.02	1.40	0.00119	0.52
	±0.00011	±0.06	±2.3	±0.008	±0.09	±0.06	±0.01	±0.00004	
HD 225137	4.33346	49326.559	–	0.000	56.42	0.94	3.36	0.0808	0.79
	±0.00002	±0.004	–	–	±0.19	±0.13	±0.01	±0.0008	

Table 2. Radial velocities and (O − C) residuals for HD 341.

Date (JD) 240 0000+	Cycle	RV km s^{-1}	(O − C) km s^{-1}
48940.41	−0.20	−24.3	0.7
48966.37	3.96	6.0	0.4
48967.34	4.12	28.5	0.5
48969.34	4.44	−6.3	0.9
48970.25	4.58	−31.2	−0.3
48970.50	4.62	−34.2	−0.1
48972.27	4.91	−6.2	−0.5
49000.31	9.40	0.1	−0.4
49002.31	9.72	−33.9	0.1
49317.49	60.21	28.0	−0.3
49318.30	60.34	12.2	−0.2
49319.32	60.50	−19.1	0.0
49320.32	60.66	−34.8	0.6
49321.33	60.82	−22.1	−0.2
49323.30	61.14	30.1	1.2
49324.49	61.33	13.9	0.1
49325.34	61.47	−12.0	0.5
49640.51	111.95	3.1	−0.4
49641.43	112.10	27.0	0.4
49642.30	112.24	26.1	0.0
49642.43	112.26	24.3	0.3
49642.52	112.27	22.5	0.3
49643.29	112.40	0.9	−0.1
49644.29	112.56	−27.0	0.7
49644.51	112.59	−31.5	0.2
50123.32	189.29	19.5	−0.2
50124.28	189.45	−8.8	−0.2
50125.27	189.60	−33.0	−0.3
50127.28	189.93	−1.1	0.7
50323.59	221.37	5.5	−0.3
50324.57	221.53	−24.2	−0.4
50325.55	221.69	−35.7	−0.3
50326.58	221.85	−16.5	0.4
50327.54	222.00	13.5	−0.2
50328.56	222.17	28.7	−0.7
50415.37	236.07	24.5	0.5
50419.52	236.74	−33.4	−0.8
50420.32	236.87	−13.7	0.2
50421.34	237.03	17.1	−0.9
50421.43	237.05	19.8	−0.6
50477.32	246.00	12.5	−0.1
50478.27	246.15	28.7	−0.6
50480.24	246.47	−13.0	−0.3
50481.27	246.63	−34.5	−0.1
51106.46	346.78	−28.7	−0.2

Table 3. Radial velocities and (O − C) residuals for HD 55822.

Date (JD) 240 0000+	Cycle	RV km s^{-1}	(O − C) km s^{-1}
48670.48	−0.61	1.7	0.5
48671.45	−0.42	35.5	0.5
48672.41	−0.23	68.8	0.6
48673.55	−0.01	48.5	−0.7
48674.41	0.16	1.0	−0.6
48674.55	0.18	−3.3	−0.9
48675.29	0.33	−5.6	−0.4
48675.55	0.38	−1.5	−1.6
48676.28	0.52	23.4	0.1
48676.55	0.57	33.5	−0.3
48936.57	51.33	−5.6	−0.6
48937.54	51.52	24.4	1.5
48937.73	51.56	29.3	−1.0
48938.52	51.71	60.6	0.1
48939.52	51.91	68.5	0.6
48940.53	52.10	14.8	0.8
48966.58	57.19	−2.5	0.5
48967.45	57.36	−2.5	0.0
48969.46	57.75	66.5	0.2
48970.45	57.94	61.7	0.6
48970.73	58.00	45.8	−0.3
48972.43	58.33	−5.9	−0.9
48999.61	63.64	44.7	−1.5
49000.55	63.82	72.6	0.2
49317.50	125.69	55.5	−0.7
49318.48	125.88	70.3	−0.7
49319.48	126.07	23.0	0.7
49320.48	126.27	−6.2	1.5
49324.58	127.07	23.1	−0.2
49325.50	127.25	−7.7	−0.2
49426.40	146.95	59.5	−1.1
49427.36	147.13	5.1	−1.3
49430.42	147.73	62.4	−1.0
49431.48	147.94	61.3	−1.2
49432.34	148.11	13.0	−0.2
49640.70	188.78	69.5	0.2
49641.71	188.97	54.1	0.6
49642.70	189.17	−0.4	−0.2
49644.68	189.56	30.1	0.2
49783.36	216.63	45.3	1.1
49784.30	216.81	73.0	1.2
49784.50	216.85	72.8	0.1
49785.44	217.03	37.6	1.3
49786.43	217.22	−4.8	1.5
49787.44	217.42	6.7	1.0
50123.50	283.02	40.7	1.2
50124.48	283.21	−5.8	−0.3
50125.51	283.41	4.3	−0.1
50192.37	296.46	12.3	−0.3
50195.33	297.04	32.5	−0.1
50415.67	340.05	27.7	−1.5
50418.49	340.60	38.6	−0.8
50477.46	352.11	11.9	0.7
50479.42	352.50	19.3	1.0

Parallaxes of the eight stars are available in the *Hipparcos* catalogue (ESA 1997). They are given in line 6 of Table 10, with their errors and the corresponding distances in line 7. From those parallaxes, we estimated the absolute magnitudes (line 8). Because all these stars are rather close to the Sun, we can neglect the interstellar absorption.

Except for the composite system HD 61250 (see above), when Strömgren indices were available (Hauck & Mermilliod 1998), we deduced the parameters $T_{\rm eff}$ and $\log g$ (lines 10 and 11) for the primary component, using the grids giving c versus β from Moon & Dworetsky (1985). When the β index was not available (in the case of HD 341 and HD 55822), we estimated its value from the straight correlation that exists between $b - y$ and β, as given by Crawford (1979). For the [Fe/H] estimation (line 12), we first computed $\delta m_1 = m_1(\text{standard}) - m_1(\text{observed})$, where m_1 (standard) was deduced from $b - y$ or β using the calibration of Crawford (1979).

Table 4. Radial velocities and (O − C) residuals for HD 61250.

Date (JD) 240 0000+	Cycle	RV km s^{-1}	(O − C) km s^{-1}
48937.68	−0.72	−10.2	−0.6
48938.70	−0.27	−8.2	0.2
48940.70	0.63	−24.1	−1.3
48967.63	12.70	−12.6	−0.1
48968.68	13.17	4.2	−2.0
48969.40	13.50	−31.5	−0.7
48969.73	13.65	−18.1	2.4
48970.39	13.94	17.8	−0.4
48970.72	14.09	17.1	1.1
48972.64	14.95	19.8	1.0
49000.59	27.49	−30.9	−0.2
49003.65	28.86	9.7	−0.7
49317.64	169.64	−21.2	0.1
49318.64	170.09	15.7	−0.2
49319.63	170.54	−28.2	1.9
49320.53	170.94	16.3	−1.9
49323.59	172.31	−12.2	2.8
49324.64	172.78	0.1	0.4
49325.56	173.19	1.5	−1.8
49325.75	173.28	−10.3	−0.4
49426.42	218.42	−29.0	−1.4
49427.31	218.82	5.5	0.6
49427.51	218.91	15.2	−0.5
49428.46	219.34	−16.6	1.8
49428.52	219.36	−19.6	2.0
49429.41	219.76	−2.7	1.5
49430.29	220.15	8.8	−0.5
49430.49	220.24	−4.2	0.1
49431.30	220.61	−25.4	−0.1
49432.29	221.05	20.3	1.5
49432.48	221.14	12.4	1.2
49783.48	378.52	−31.5	−0.9
49784.31	378.89	13.3	−0.9
49785.43	379.39	−23.0	2.0
49787.29	380.23	−1.5	0.1
50123.51	530.98	21.3	1.6
50124.54	531.44	−29.9	−0.7
50125.47	531.86	11.8	0.9
50127.54	532.79	−0.1	−0.7
50193.52	562.37	−22.4	0.9
50415.59	661.94	17.1	−1.3
50416.52	662.36	−22.3	−0.7
50418.39	663.20	0.4	−1.9
50479.43	690.57	−30.4	−1.9
50479.60	690.64	−22.3	−1.3
50480.58	691.08	16.1	−0.4
50481.49	691.49	−33.0	−2.2
50836.53	850.69	−13.8	1.3
50839.49	852.01	20.4	0.5

Table 5. Radial velocities and (O − C) residuals for HD 67317.

Date (JD) 240 0000+	Cycle	RV km s^{-1}	(O − C) km s^{-1}
49320.55	−0.11	32.1	0.3
49323.60	0.58	−23.6	−0.4
49324.63	0.81	18.2	−0.1
49325.63	1.03	38.4	−0.4
49426.44	23.77	11.2	−0.1
49427.43	24.00	40.2	0.6
49427.57	24.03	40.2	1.1
49428.32	24.20	16.5	−0.6
49428.50	24.24	8.2	−0.6
49429.39	24.44	−23.2	1.3
49429.52	24.47	−27.1	−0.9
49430.30	24.64	−14.8	−0.7
49430.53	24.70	−4.8	−0.2
49431.31	24.87	29.5	0.0
49431.57	24.93	37.3	0.7
49432.30	25.10	33.5	−0.3
49432.54	25.15	26.9	0.7
49642.69	72.55	−25.1	0.0
49643.68	72.78	11.7	0.1
49644.68	73.00	39.8	0.2
49781.40	103.84	26.3	1.9
49781.56	103.88	30.6	0.3
49783.39	104.29	−1.1	1.1
49783.57	104.33	−9.0	0.8
49784.44	104.53	−26.0	0.4
49785.32	104.73	2.4	1.1
49786.44	104.98	39.1	−0.2
49787.47	105.21	14.8	0.2
50124.51	181.24	9.1	0.0
50125.39	181.44	−24.5	−0.3
50126.54	181.69	−5.9	−0.7
50127.53	181.92	35.0	−0.3
50193.45	196.79	13.2	−0.6
50414.55	246.66	−11.4	−0.1
50415.60	246.90	32.3	−0.5
50416.57	247.12	29.8	−1.5
50418.71	247.60	−20.9	−0.4
50419.66	247.81	18.6	−0.4
50420.71	248.05	36.1	−1.8
50479.45	261.30	−3.8	0.0
50479.70	261.36	−14.2	0.1
50480.36	261.50	−27.7	−0.9
50481.44	261.75	6.0	0.0
50834.52	341.39	−18.9	0.5
50835.60	341.64	−15.0	0.4
50836.46	341.83	22.7	0.1

Then we used the δm_1 versus [Fe/H] relation given by Crawford (1975).

For HD 67317, 162950, 224890 and 225137, Geneva photometry was available (Burki et al. 2003); we could use the calibration of Kunzli et al. (1997) for all those objects except for HD 67317, which appeared outside Kunzli's calibration grids. A possible explanation for this discrepancy could be a photometric perturbation from the secondary spectroscopic component. The effective temperature of HD 67317 given in Table 10 was estimated from the *B–V* index and the calibration table of Flower (1996). For HD 162950, because photometry was available both in Strömgren and Geneva systems, we give the mean values of those physical parameters in Table 10.

Finally, we report in Fig. 4 the positions of the eight primaries in the theoretical Hertzsprung–Russell (HR) diagram from Schaller et al. (1992), completed with the isochrones computed by Meynet, Mermilliod & Maeder (1993). The values of the absolute luminosity L come from those of M_v (Table 10) via the bolometric corrections tabulated by Schmidt-Kaler. The positions of the stars in this HR diagram lead to *theoretical* estimates of their masses M_1 and ages (lines 14 and 17 of Table 10), and give an idea of their evolutionary

Table 6. Radial velocities and (O − C) residuals for HD 93991.

Date (JD) 240 0000+	Cycle	RV km s^{-1}	(O − C) km s^{-1}
48672.56	−0.76	−15.7	−1.6
48673.61	−0.43	−30.2	0.2
48674.53	−0.15	−5.0	0.5
48674.71	−0.09	−0.7	0.8
48675.39	0.12	−4.3	−0.9
48675.71	0.22	−11.1	1.2
48676.39	0.43	−28.8	1.5
48676.69	0.52	−31.0	0.6
48940.71	82.81	−10.2	−0.8
48967.73	91.23	−14.8	−1.3
48968.70	91.53	−30.7	0.7
48969.63	91.82	−10.0	−1.9
48970.69	92.15	−7.0	−1.0
49000.66	101.50	−30.8	1.0
49140.35	145.03	1.2	0.4
49141.34	145.34	−23.3	0.8
49143.37	145.97	1.2	0.4
49144.44	146.30	−19.4	1.4
49145.37	146.60	−29.1	−0.2
49146.41	146.92	0.1	1.1
49147.36	147.22	−12.2	−0.4
49148.37	147.53	−32.4	−0.9
49317.65	200.29	−20.2	−0.9
49318.71	200.62	−27.6	−0.1
49320.62	201.21	−11.8	−0.1
49323.68	202.17	−6.9	0.4
49324.71	202.49	−31.6	0.1
49325.71	202.80	−9.9	0.3
49325.72	202.80	−9.8	0.0
49427.45	234.51	−32.2	−0.4
49428.36	234.79	−11.7	−0.6
49429.38	235.11	−2.2	0.5
49430.35	235.41	−27.6	1.7
49431.42	235.75	−16.9	−1.2
49432.50	236.08	−1.7	−0.7
49781.55	344.87	−2.2	1.9
49785.52	346.11	0.0	2.5
49787.48	346.72	−18.7	0.1
50124.60	451.79	−11.4	0.3
50125.54	452.08	−0.3	0.5
50126.57	452.40	−29.1	−0.4
50127.56	452.71	−18.1	1.5
50193.37	473.22	−12.5	−0.5
50193.54	473.27	−19.4	−2.0
50194.46	473.56	−29.8	0.8
50414.68	542.19	−8.1	1.6
50479.46	562.38	−28.2	−0.7
50479.65	562.44	−30.5	0.2
50480.47	562.70	−22.0	−1.3
50481.53	563.03	0.6	−0.3
50609.42	602.89	−3.6	−0.7
50614.39	604.44	−31.5	−1.1
50746.70	645.67	−24.6	−1.3
50837.56	673.99	0.6	−0.5
50976.37	717.25	−16.3	−0.9

status. Five stars, namely HD 55822, 61250, 67317, 162950 and 224890, are little evolved bona fide dwarfs, while the three others are already evolved in the main sequence. In Table 10, we also give the *theoretical* radius R_1 (line 13), calculated from the L and T_{eff}

Table 7. Radial velocities and (O − C) residuals for HD 162950.

Date (JD) 240 0000+	Cycle	RV km s^{-1}	(O − C) km s^{-1}
49145.52	−0.83	17.0	−0.7
49146.50	−0.74	17.4	−0.6
49427.70	27.26	18.6	0.6
49431.69	27.66	1.1	0.2
49640.29	48.43	11.9	−0.4
49641.30	48.53	7.7	0.2
49642.30	48.63	2.1	−0.2
49643.30	48.73	−2.8	−0.4
49644.33	48.83	−5.5	−0.2
49781.72	62.51	8.1	−0.2
49782.70	62.61	2.9	−0.5
49783.71	62.71	−1.5	0.1
49785.67	62.91	−3.7	0.3
49786.65	63.00	4.2	−0.4
49787.70	63.11	14.7	−0.2
50193.60	103.53	7.5	−0.2
50194.57	103.62	3.4	0.6
50195.59	103.72	−2.3	−0.2
50324.39	116.55	6.3	−0.3
50325.40	116.65	1.4	0.0
50326.43	116.75	−3.3	0.0
50327.41	116.85	−5.7	−0.4
50328.31	116.94	−1.9	0.0
50329.45	117.05	10.0	0.0
50414.25	125.50	8.9	−0.3
50418.27	125.90	−4.8	−0.4
50419.23	125.99	3.7	0.5
50420.24	126.09	13.5	−0.2
50611.48	145.14	17.0	0.5
50614.57	145.44	11.7	0.0
50739.27	157.86	−5.0	0.3
50740.31	157.96	0.1	0.0
50745.30	158.46	11.1	0.2
50746.34	158.56	6.1	0.3
50927.64	176.62	2.7	−0.4
50931.59	177.01	4.6	−0.5
50944.62	178.31	17.1	0.1
50945.57	178.40	13.8	0.2
50947.52	178.60	4.6	0.5
50974.61	181.29	17.4	0.1
50975.53	181.38	14.1	−0.2
50977.52	181.58	4.5	−0.3
50978.50	181.68	0.0	0.1
50979.54	181.78	−4.9	−0.5
50990.48	182.87	−5.0	0.1
50991.48	182.97	0.7	−0.4
50992.50	183.07	12.3	0.1
50993.41	183.17	17.2	−0.5
50994.41	183.26	18.0	0.0
50997.43	183.57	5.6	−0.1
50998.41	183.66	1.1	0.4
50999.46	183.77	−3.7	0.1
51000.43	183.86	−5.2	0.0
51001.41	183.96	0.3	0.3
51032.38	187.05	9.8	0.6
51033.37	187.14	17.6	0.7
51035.36	187.34	15.4	−0.5
51036.35	187.44	12.1	0.3
51037.35	187.54	7.2	0.2
51090.28	192.81	−4.1	0.9
51105.30	194.31	17.4	0.4
51108.31	194.61	3.5	−0.1
51117.27	195.50	9.5	0.4
51123.23	196.09	13.7	0.0

Table 8. Radial velocities and (O − C) residuals for HD 224890.

Date (JD) 240 0000+	Cycle	RV km s^{-1}	(O − C) km s^{-1}
44485.55	−469.88	−16.6	0.7
44558.34	−462.25	2.2	0.5
45198.57	−395.19	2.2	−0.8
48970.32	−0.09	0.8	−0.2
48972.31	0.12	−16.8	0.2
49000.30	3.05	−12.7	−0.6
49002.37	3.27	−18.0	−0.2
49317.36	36.26	−17.3	0.6
49318.34	36.36	−13.8	0.7
49319.35	36.47	−10.2	−0.2
49320.30	36.57	−4.5	1.0
49321.34	36.68	−0.1	0.7
49323.29	36.88	2.2	0.0
49324.48	37.01	−7.2	0.6
49325.32	37.10	−15.5	0.3
49640.50	70.11	−16.8	−0.1
49641.40	70.20	−18.4	0.3
49642.29	70.30	−17.3	−0.4
49642.52	70.32	−15.6	0.5
49643.27	70.40	−13.9	−0.9
49643.52	70.43	−11.9	0.0
49644.30	70.51	−7.8	0.5
49644.60	70.54	−7.3	−0.4
50123.30	120.68	−0.9	−0.4
50124.29	120.79	3.6	0.9
50125.29	120.89	1.8	0.0
50127.26	121.10	−15.6	0.5
50324.53	141.76	1.9	−0.2
50325.53	141.87	2.1	−0.5
50326.56	141.98	−4.7	−0.2
50327.52	142.08	−14.9	−0.4
50328.52	142.18	−18.0	0.7
50329.56	142.29	−16.9	0.2
50416.43	151.39	−11.8	1.6
50418.45	151.60	−4.7	−0.7
50419.53	151.72	0.4	−0.2
50420.45	151.81	3.6	0.6
50421.44	151.92	0.6	0.0
50476.27	157.66	−0.7	0.9
50478.25	157.87	3.0	0.4
50479.24	157.97	−3.8	0.1
50615.61	172.25	−18.7	−0.7
50738.49	185.13	−17.5	0.0
50741.56	185.45	−10.5	0.5
50745.40	185.85	3.2	0.3
50746.38	185.95	−2.1	0.2
50837.34	195.48	−10.0	−0.5
50977.60	210.17	−19.3	−0.7
51032.56	215.93	−0.2	0.3
51033.57	216.04	−11.0	0.0
51034.58	216.14	−18.2	−0.2
51035.57	216.25	−18.2	0.0
51036.57	216.35	−15.5	−0.5
51037.56	216.46	−11.0	−0.3
51090.43	221.99	−6.6	−0.3
51109.54	223.99	−6.3	0.1
51111.41	224.19	−19.7	−1.0
51117.40	224.82	2.7	−0.3
51119.39	225.03	−10.5	−0.6
51123.38	225.44	−11.2	−0.1
51147.37	227.96	−2.3	0.4
51148.29	228.05	−12.6	0.0

Table 8 – *continued*

Date (JD) 240 0000+	Cycle	RV km s^{-1}	(O − C) km s^{-1}
51149.37	228.17	−18.8	−0.3
51150.30	228.26	−17.7	0.1
51151.31	228.37	−14.3	0.0
51152.29	228.47	−10.6	−0.7
51153.32	228.58	−5.0	0.0
51154.27	228.68	−1.0	−0.3
51155.30	228.79	1.9	−0.8
51156.32	228.89	1.3	−0.4
51158.30	229.10	−16.2	0.1
51161.25	229.41	−12.0	0.6
51162.31	229.52	−8.6	−1.0
51212.26	234.76	1.9	0.0

Table 9. Radial velocities and (O − C) residuals for HD 225137.

Date (JD) 240 0000+	Cycle	RV km s^{-1}	(O − C) km s^{-1}
49323.39	−0.73	−3.8	1.9
49325.33	−0.28	−10.4	0.6
49640.57	72.46	−54.3	−0.5
49641.41	72.66	−30.1	0.4
49641.66	72.71	−12.1	−0.2
49642.28	72.86	35.5	−0.3
49642.51	72.91	48.9	0.5
49643.27	73.08	49.9	0.2
49643.55	73.15	33.7	−0.7
49644.28	73.32	−23.0	−0.4
49644.43	73.35	−33.5	−0.8
49644.59	73.39	−43.1	−0.5
50123.31	183.86	37.8	0.7
50124.27	184.08	50.2	0.1
50125.28	184.32	−21.2	0.3
50127.27	184.77	9.2	−0.2
50324.55	230.30	−16.7	−0.8
50325.54	230.53	−56.6	−1.9
50326.57	230.77	5.5	−0.8
50327.52	230.99	56.2	−0.9
50328.55	231.22	10.0	−1.1
50329.64	231.47	−54.2	0.5
50414.50	251.06	54.8	0.8
50415.38	251.26	−0.8	1.1
50416.39	251.49	−55.0	0.4
50418.35	251.94	54.0	0.0
50419.35	252.18	26.3	−0.1
50419.45	252.20	18.6	−0.1
50420.37	252.41	−46.7	0.0
50420.55	252.45	−53.1	−0.2
50421.25	252.61	−42.2	−0.7
50476.36	265.33	−26.2	0.6
50477.34	265.56	−52.4	−0.4
50478.36	265.79	15.4	−0.4
50479.34	266.02	57.4	0.4
50480.23	266.22	9.2	−0.6
50482.24	266.69	−20.9	−0.2
50739.37	326.02	56.8	0.0
50746.39	327.64	−32.6	1.6
50810.29	342.39	−40.3	2.1
50831.23	347.22	10.2	−1.0
51032.58	393.69	−22.2	−0.8
51106.46	410.74	−3.3	0.9
51109.45	411.42	−48.4	0.6

Table 10. Estimated physical parameters from observational data and theoretical statements. An asterisk * was added when pseudo-synchronism was involved instead of genuine synchronism (in the case of non-circular orbits).

HD HIP	341 659	55822 35086	61250 37604	67317 40006	93991 53119	162950 87486	224890 128	225137 303
V	7.27	8.53	8.23	7.56	8.09	7.29	6.50	8.13
B–V	0.21	0.30	0.23	0.27	0.29	0.29	0.18	0.32
$v \sin i$	11.7 ± 1.0	21.0 ± 1.0	25.2 ± 1.0	12.6 ± 1.0	26.2 ± 1.0	8.8 ± 1.0	11.9 ± 1.0	19.1 ± 1.0
π	4.90 ± 0.76	6.08 ± 1.68	6.05 ± 1.60	11.03 ± 1.46	3.85 ± 0.91	11.65 ± 0.70	15.20 ± 0.63	5.15 ± 0.98
d (pc)	204^{+38}_{-27}	164^{+63}_{-35}	165^{+60}_{-34}	91^{+13}_{-11}	260^{+80}_{-50}	86^{+5}_{-5}	66^{+3}_{-3}	194^{+46}_{-31}
M_v	0.72 ± 0.33	2.45 ± 0.61	2.40 ± 0.56	2.77 ± 0.28	1.02 ± 0.52	2.62 ± 0.13	2.41 ± 0.09	1.69 ± 0.41
$\log L/L_\odot$	1.67 ± 0.13	0.96 ± 0.24	0.98 ± 0.22	0.83 ± 0.11	1.53 ± 0.21	0.89 ± 0.05	0.99 ± 0.04	1.26 ± 0.16
$T_{\rm eff}$ (K)	8100 ± 80	7300 ± 75	7600 ± 75	7400 ± 75	7600 ± 75	7400 ± 75	8100 ± 80	7200 ± 75
$\log g$ (cgs)	3.90	4.00	–	–	4.00	4.24	4.50	3.65
[Fe/H]	+0.60	+0.91	–	–	+0.76	+0.40	+0.22	+0.41
$R_1/R_\odot$	3.6 ± 0.2	2.0 ± 0.2	1.9 ± 0.2	1.7 ± 0.1	3.5 ± 0.2	1.7 ± 0.1	1.7 ± 0.1	2.9 ± 0.2
$M_1/M_\odot$	2.30 ± 0.20	1.65 ± 0.20	1.70 ± 0.15	1.60 ± 0.10	2.20 ± 0.20	1.60 ± 0.05	1.75 ± 0.05	1.90 ± 0.15
$M_{2\,\rm min}/M_\odot$	0.57	0.55	0.24	0.41	0.21	0.17	0.16	0.85
$a/R_\odot$	23 ± 3	18 ± 3	10 ± 2	16 ± 2	14 ± 2	27 ± 4	27 ± 4	18 ± 3
log age (yr)	$8.80^{+0.03}_{-0.05}$	$9.00^{+0.03}_{-0.4}$	$8.90^{+0.07}_{-0.3}$	$8.75^{+0.2}_{-0.15}$	$8.90^{+0.05}_{-0.1}$	$8.90^{+0.05}_{-0.1}$	~ 8.6	$9.03^{+0.04}_{-0.06}$
$\log t_{\rm sync}$ (yr)	4.66	5.59	4.73	5.51	4.48	6.99	7.11	4.50
$\sin i_{\rm sync}$	$0.401 \pm .057$	$0.975 \pm .144$*	$0.585 \pm .085$	$0.649 \pm .090$	$0.475 \pm .045$	$0.827 \pm .143$*	1.04 ± 0.15*	$0.564 \pm .068$
$\mu_{\rm sync}$	0.78 ± 0.20	0.34 ± 0.08	0.26 ± 0.06	0.43 ± 0.10	0.21 ± 0.04	0.13 ± 0.03	0.094 ± 0.016	0.97 ± 0.22

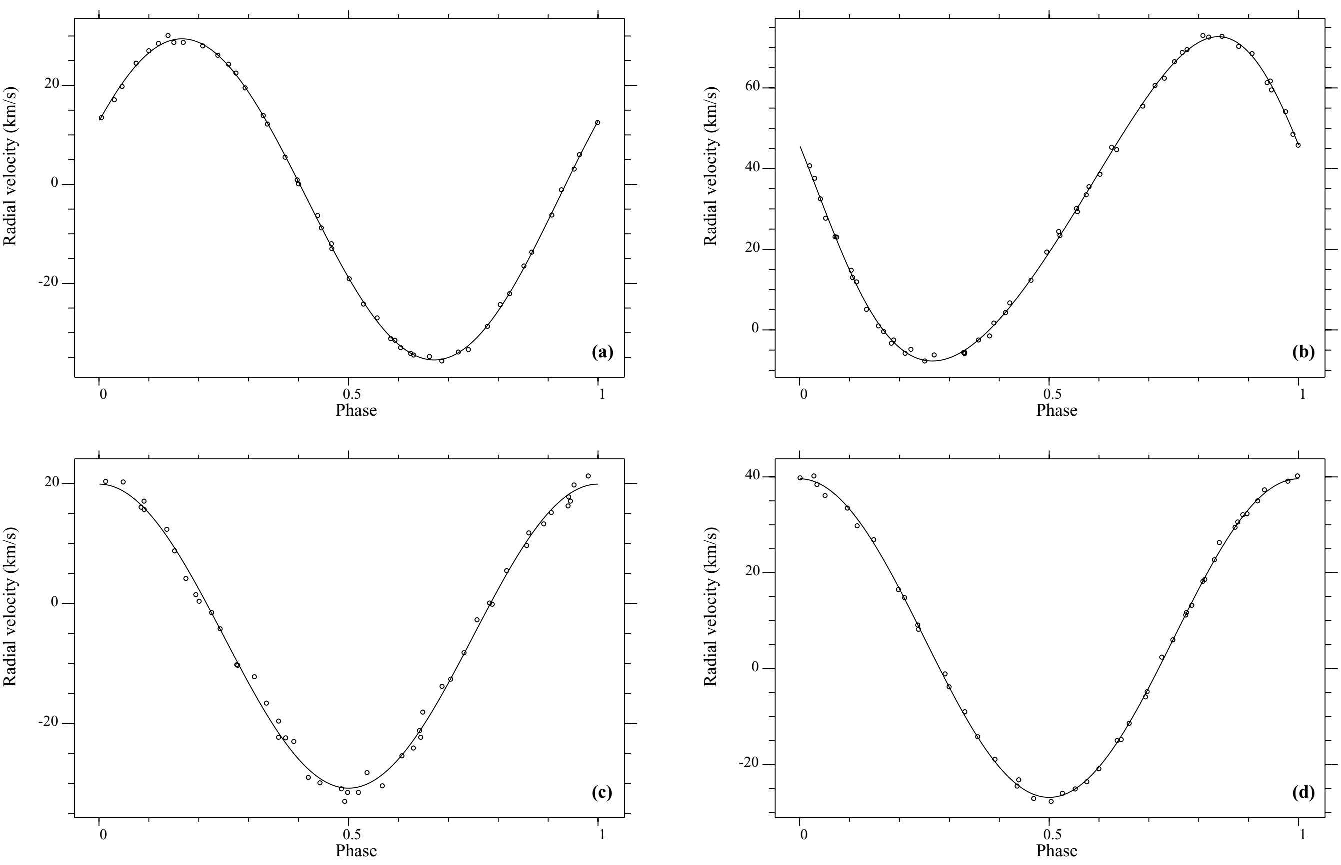

Figure 2. RV curves computed with the orbital elements of Table 1: (a) HD 341, (b) HD 55822, (c) HD 61250 and (d) HD 67317. For HD 61250 and HD 67317, which have a circular orbit, the ascending node is taken as the origin of the phases. For the other systems, the origin of the phases corresponds to the periastron passage.

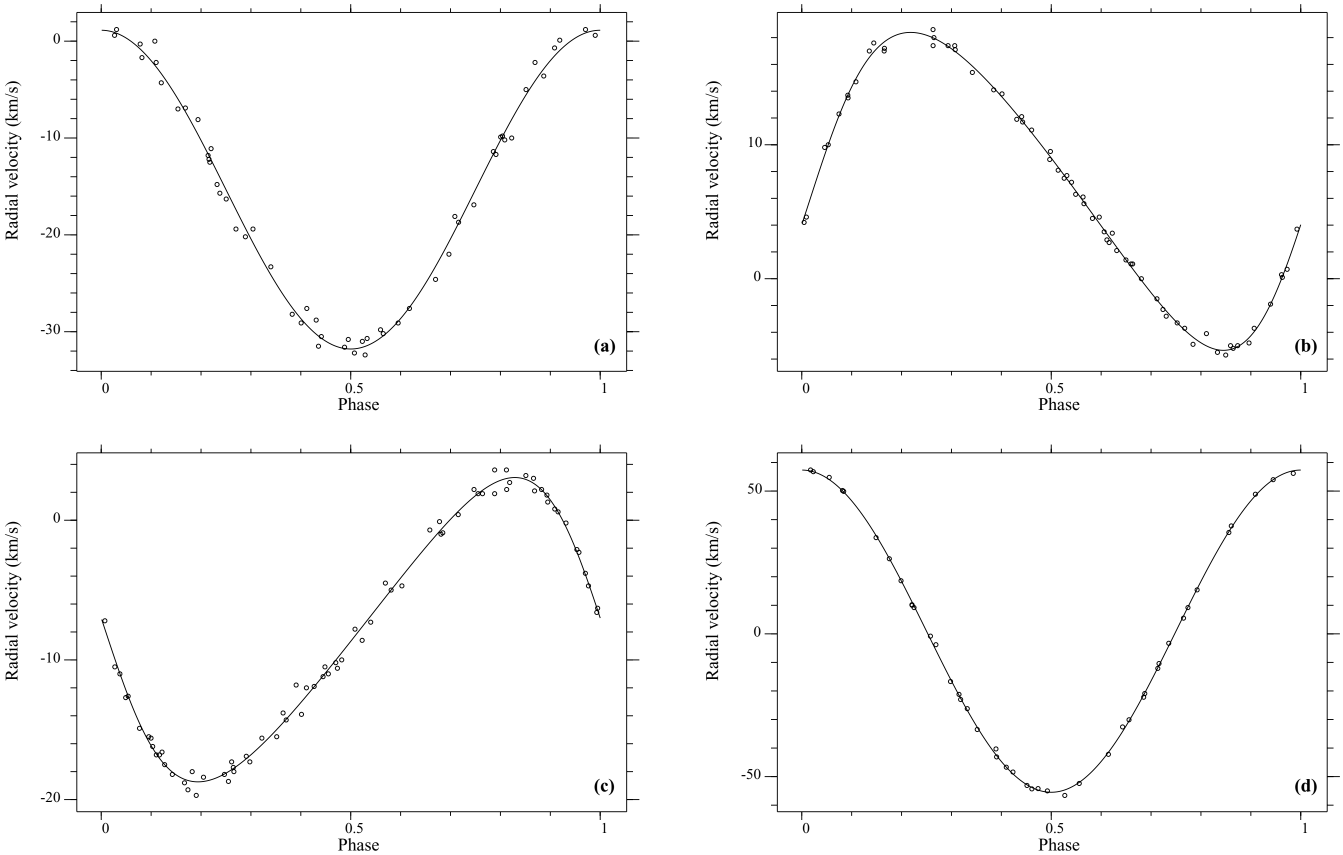

Figure 3. RV curves computed with the orbital elements of Table 1: (a) HD 93991, (b) HD 162950, (c) HD 224890 and (d) HD 225137. For HD 93991 and HD 225137, which have a circular orbit, the ascending node is taken as the origin of the phases. For the other systems, the origin of the phases corresponds to the periastron passage.

values. These estimates will be used for the study of synchronism (Section 4.3).

4.2 Minimum masses and separations of the secondaries

Using the mass function derived from the orbits (Table 1) and the theoretical value found for M_1, the mass of the primary (see above), we can estimate the minimum mass $M_{2\min}$ of the unseen spectroscopic companion. The mass function can be written as

$$f(m) = M_1 \times \sin^3 i \times \mu^3/(1+\mu)^2, \quad (1)$$

where $\mu = M_2/M_1$ is the mass ratio in the system.

The value of i is unknown, and $M_{2\min}$ is obtained for $\sin i = 1$. Except for HD 225137, the corresponding masses are those of red dwarfs of type K or M (cf. line 15 of Table 10).

We can then estimate the mean separation a for each system from the values of $a_1 \sin i$ obtained in Table 1:

$$a = a_1 + a_2 = (a_1 \sin i) \times (1 + 1/\mu)/\sin i. \quad (2)$$

As pointed out by Carquillat et al. (1982) in the case of SB1s, the separations we obtain have a small dependence on the value chosen for i. Let a_0 be the separation assuming $i = 90^\circ$, and a the true separation. The ratio a/a_0 may be approximated by the function $(\sin i)^{-1/4}$. More precisely, this is an upper estimation. Hence, when i decreases from 90° to 20° (the most probable range for SBs, with a corresponding probability of 94 per cent), a increases by less than 30 per cent of its initial value, a_0. The separations we obtain (line 16 of Table 10) are a few tens of solar radii; hence, those systems are detached binaries.

4.3 Rotation-revolution synchronism

Synchronization of a binary system is a powerful process for slowing the axial rotation of a star. It seems established that such a slow rotation is required to form Am stars through the diffusion of chemical elements (Michaud et al. 1983).

Tidal interaction in close detached binaries can lead either to a spiralling in of the two stars followed by a collision, or to the evolution towards an equilibrium state, characterized by coplanarity, circularity and corotation. In the last case, the orbital parameters will asymptotically reach their equilibrium values, but on different time-scales. In particular, it is expected that the rotation of each component quickly synchronizes with the instantaneous orbital angular velocity at periastron. This state is called 'pseudo-synchronization' (Hut 1981). Pseudo-synchronization is caused by the fact that tidal interaction is strongest around periastron.

Among the different mechanisms that have been proposed to account for the evolution toward synchronism in binary systems, large-scale meridional flows (Tassoul 1987) seem the most effective for early-type stars. They could also account for the diffusion of chemical elements and explain the correlation between slow rotation and abnormal spectrum for Hg–Mn and Fm–Am stars (Charbonneau &

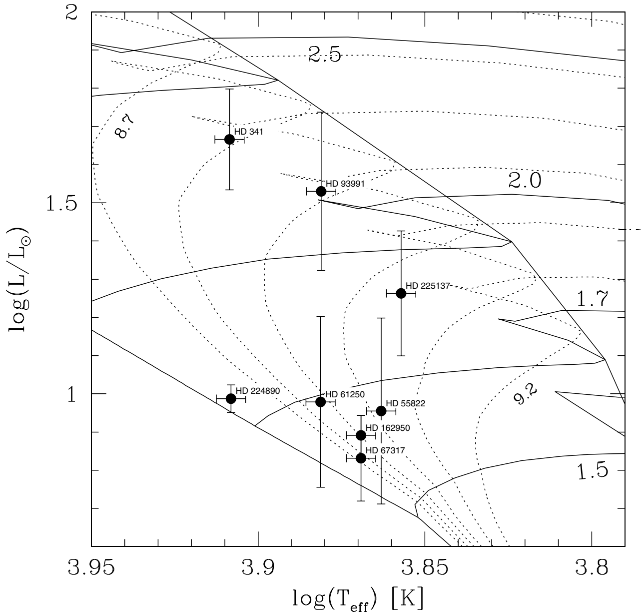

Figure 4. Location of the primary components in the theoretical evolutionary HR diagram computed by Schaller et al. (1992), with the isochrones (dotted lines) given by Meynet et al. (1993), for log age (years) varying from 8.7 to 9.2 by steps of 0.1. The solid lines correspond to the evolution tracks for mass values of 1.5, 1.7, 2.0 and 2.5 $M_{\odot}$.

Michaud 1988). The corresponding characteristic time for synchronization is given by

$$t_{\rm sync} = \frac{1.44 \times 10^{-N/4}}{\mu(1+\mu)^{3/8}} \left(\frac{L}{\rm L_{\odot}}\right)^{-1/4} \left(\frac{M}{\rm M_{\odot}}\right)^{-1/8} \times \left(\frac{R}{\rm R_{\odot}}\right)^{9/8} \left(\frac{a}{R}\right)^{33/8} \quad (3)$$

where $t_{\rm sync}$ is the spin-down time expressed in years, and N is a constant, such that 10^N is the mean value of the Reynolds number $R_{\rm e}$ in the star. Let us recall that $R_{\rm e} = \mu_{\rm v}/\mu_{\rm r}$, where $\mu_{\rm v}$ and $\mu_{\rm r}$ are the coefficients of the eddy viscosity and of the radiative viscosity, respectively. For early-type binaries, the eddy viscosity is small and N may be taken equal to zero (Tassoul 1988). In the context of meridional flows, the circularization characteristic time $t_{\rm circ}$ is longer than $t_{\rm sync}$ (Tassoul 1988), which may explain the existence of (pseudo-)synchronized systems with a non-circular orbit.

The corresponding values of $t_{\rm sync}$ computed for the systems of our sample (line 18 of Table 10) are smaller than the theoretical age of the stars. This is a good indication that these stars may have reached the synchronization state (or the pseudo-synchronization state in the case of the systems with a still non-negligible eccentricity).

If we thus assume that the components rotate in synchronism with the orbital motion (corotation), and also that the equatorial plane of a star is equal to its orbital plane (coplanarity), we have the relation

$$R = \frac{V_{\rm e} P}{50.6} = \frac{V_{\rm e} \sin i \, P}{50.6 \sin i} \quad (4)$$

where $V_{\rm e}$ is the tangential equatorial velocity in km s^{-1}, P is the orbital period in days, and R is the star radius in solar radii. Indeed we only have access to the projected rotational velocity $V_{\rm e} \sin i$ (commonly called $v \sin i$), deduced from the CORAVEL correlation dips (see Benz & Mayor 1981, 1984), and given in line 5 of Table 10. Notice that for the systems with a significant eccentricity ($e > 0.1$), such as HD 55822, 162950 and 224890, we must take into account the pseudo-synchronous rotation period (see Hut 1981, formulae 44 and 45) instead of the orbital period. For these three stars, the pseudo-synchronous rotation periods are 4.70, 8.08 and 7.53 d, respectively.

For each binary, we computed the values of $\sin i_{\rm sync}$ from the preceding formula, i.e. $\sin i_{\rm sync} = P \times v \sin i/(50.6R)$, using the theoretical estimates for R given in Table 10 (line 19). It can be seen that for all systems, except for HD 224890, the values of $\sin i_{\rm sync}$ we obtained are plausible. Taking into account the uncertainties, the corresponding inclination values lie in the range 20°–90°. For HD 224890, we found an aberrant value of 1.04, which seems to indicate the absence of synchronism. It is also the youngest and the least evolved system of our sample and could have not yet reached its equilibrium state. Nevertheless, the corresponding uncertainty is ± 0.15, and we may consider that the marginal discrepancy is not definitive. For the other seven stars, we thus conclude that synchronism (or pseudo-synchronism for the eccentric orbits) is plausible.

Assuming that all systems are synchronized, we can derive the mass ratio $\mu_{\rm sync}$ from the mass function values of Table 1 with relation (1). The resulting values (line 20 of Table 10) have a wide range from $\sim$0.1 to $\mu_{\rm sync} = 0.97 \pm 0.22$ for HD 225137. This system also has the largest mass function in our sample (column 9 of Table 1). Such a high value for the mass ratio would imply that the companion could also be an A-type star. Note that it cannot be an Am star because, in that case, CORAVEL would have detected two correlation dips. If we take into account the uncertainties on the value of $\mu_{\rm sync}$, the mass of the secondary of HD 225137 could go down to $\sim$1.4 $M_{\odot}$ (lowest value at 1σ), which corresponds to a spectral type of $\sim$F5V (Schmidt-Kaler 1982). The resulting magnitude difference would be $\Delta m_v \sim 1.8$, which could account for the non-detection of the secondary with CORAVEL. Further high-resolution spectroscopic observations of HD 225137 are thus required to investigate this problem.

ACKNOWLEDGMENTS

This paper is based on observations made at the Haute-Provence Observatory (France). We are indebted to M. Mayor, Director of Geneva Observatory, for giving us observing time with CORAVEL, and to S. Udry for reducing our observations in the RV Geneva data base. We thank the referee, T. Mazeh, for his constructive comments about this paper. For bibliographic references, we used the SIMBAD data base, operated by the Centre de Données Astronomiques de Strasbourg (France).

REFERENCES

Baranne A., Mayor M., Poncet J. L., 1979, Vistas Astron., 23, 279
Benz W., Mayor M., 1981, A&A, 93, 235
Benz W., Mayor M., 1984, A&A, 138, 183
Burki G., Cramer N., Nicolet B. et al., 2003, http://obswww.unige.ch/gcpd/ph13.html
Carquillat J.-M., Nadal R., Ginestet N., Pédoussaut A., 1982, A&A, 115, 23
Carquillat J.-M., Ginestet N., Prieur J.-L., 2001, A&A, 369, 908
Carquillat J.-M., Ginestet N., Prieur J.-L., Udry S., 2002, MNRAS, 336, 1043
Charbonneau P., Michaud G., 1988, ApJ, 327, 809
Crawford D. L., 1975, AJ, 80, 955
Crawford D. L., 1979, AJ, 84, 1858
ESA, 1997, The Hipparcos and Tycho Catalogues. ESA SP-1200, ESA Publications Division, Noordwijk
Fabricius C., Makarov V. V., 2000, A&A, 356, 141
Flower P. J., 1996, ApJ, 469, 355

Ginestet N., Carquillat J.-M., 1998, A&AS, 130, 415
Ginestet N., Prieur J.-L., Carquillat J.-M., Griffin R. F., 2003, MNRAS, 342, 61
Grenier S. et al., 1999, A&AS, 137, 451
Hauck B., 1986, A&AS, 64, 21
Hauck B., Mermilliod J.-C., 1998, A&AS, 129, 431
Hut P., 1981, A&A, 99, 126
Kunzli M., North P., Kurucz R. L., Nicolet B., 1997, A&AS, 122, 51
Lucy L. B., Sweeney M. A., 1971, AJ, 76, 544
Meynet G., Mermilliod J.-C., Maeder A., 1993, A&AS, 98, 477
Michaud G., Tarasick D., Charland Y., Pelletier C., 1983, ApJ, 269, 239
Moon T. T., Dworetsky M. M., 1985, MNRAS, 217, 305
Nadal R., Ginestet N., Carquillat J.-M., Pédoussaut A., 1979, A&AS, 35, 203
Schaller G., Schaerer D., Meynet G., Maeder A., 1992, A&AS, 96, 269
Schmidt-Kaler Th., 1982, in Schaifers K., Voigt H. H., eds, Landolt-Börnstein, Numerical Data and Functional Relationships in Science and Technology. New Series, Gr. VI, Vol. 2-b, Springer-Verlag, Berlin, pp. 1–35 and 449–456
Tassoul J.-L., 1987, ApJ, 322, 856
Tassoul J.-L., 1988, ApJ, 324, L71
Udry S., Mayor M., Queloz D., 1999, in Precise Stellar Radial Velocities. ASP Conf. Ser. Vol. 185. Astron. Soc. Pac., San Francisco, p. 367

This paper has been typeset from a TEX/LATEX file prepared by the author.